Published in final edited form as:
Immunity. 2011 August 26; 35(2): 194–207. doi:10.1016/j.immuni.2011.05.016.

Innate immune recognition of an AT-rich stem-loop DNA motif in the *Plasmodium falciparum* genome

Shruti Sharma[1], **Rosane B. DeOliveira**[1,§], **Parisa Kalantari**[1,§], **Peggy Parroche**[1], **Nadege Goutagny**[1], **Zhaozhao Jiang**[1], **Jennie Chan**[1], **Daniella C. Bartholomeu**[2], **Fanny Lauw**[1], **J. Perry Hall**[3], **Glen N. Barber**[4], **Ricardo T. Gazzinelli**[1,2,5], **Katherine A. Fitzgerald**[1,#], and **Douglas T. Golenbock**[1,#]

[1]Division of Infectious Diseases and Immunology, Department of Medicine, University of Massachusetts Medical School, 364 Plantation Street, Worcester, MA 01605, USA

[2]Department of Parasitology and Department of Biochemistry and Immunology, Biological Sciences Institute, Federal University of Minas Gerais, Av. Antonio Carlos 6627, Belo Horizonte, MG 31270, Brazil

[3]Department of Inflammation and Remodeling, Pfizer, Cambridge, MA 02140

[4]University of Miami School of Medicine, Division of Hematology and Oncology, Department of Medicine, 1550 Northwest 10th Avenue (M710), Papanicolaou Building, Room 511, Miami, FL 33136, USA

[5]Laboratory of Immunopathology, René Rachou Institute, Oswaldo Cruz Foundation, Av. Augusto de Lima 1715, Belo Horizonte, MG 30190, Brazil

SUMMARY

Although Toll-like receptor 9 (TLR9) has been implicated in regulating cytokine and type I interferon (IFN) production during malaria in humans and mice, the high AT content of the *Plasmodium falciparum* genome prompted us to examine the possibility that malarial DNA triggered TLR9-independent DNA sensing pathways. Over 6000 ATTTTTAC ("AT-rich") motifs are present in the genome of *P. falciparum*, which we show here potently induce type I IFNs. Parasite DNA, parasitized erythrocytes and oligonucleotides containing the AT-r motif induce type I IFNs via a pathway that did not involve previously described sensors including TLR9, DAI, RNA polymerase-III or IFI16/p204. Rather, AT-rich DNA sensing involved an unknown receptor that coupled to STING, TBK1 and IRF3-IRF7 signaling pathway. Mice lacking both IRF3 and IRF7, the kinase TBK1 or the type I IFN receptor were resistant to otherwise lethal cerebral

Correspondence and requests for materials should be addressed to K.A.F, kate.fitzgerald@umassmed.edu or D.T.G, douglas.golenbock@umassmed.edu.
§ and #are equal contributors

Author Contributions;

K.A.F and D.T.G oversaw the whole project with R.T.G and S.S. S.S. designed and conducted the experiments with help from Z.J., R.D., P.P. P.K. F.L. and N.G. D.C.B quantified the AT-r and CpG motif frequency, R.O. and J.C. conducted the *in vivo* mouse models and H.B. performed microarray analysis. G.B. made sting-deficient mice and J.P.H made the TBK1-hypomorphic mice. S.S., K. A. F. and D.T.G wrote the manuscript.

Competing financial interest.

The authors declare no competing financial interest.

malaria. Collectively, these observations implicate AT-rich DNA sensing via STING, TBK1 and IRF3-IRF7 in *P. falciparum* malaria.

INTRODUCTION

Malaria is the world's most common infectious disease, affecting approximately 250 million people annually with close to 1 million deaths, mainly in children. Recurrent infections for individuals living in endemic malarial regions are common because the disease does not promote strong acquired immunity. While a combination of vector control and therapy has eliminated malaria from the wealthy countries of the world, vaccine development remains a major goal for eradication of malaria in underdeveloped countries. Much is known about the acquired immune responses to both the natural *Plasmodium* infection and a variety of immunogens (Clark et al., 2004). In contrast, little is known about the innate immune response during malaria.

The life cycle of *Plasmodium falciparum* begins in the liver. After initial replication, the parasite bursts from hepatocytes and infects erythrocytes, where cycles of asexual replication occur. The cyclic rupture of parasitized erythrocytes releases one or more malarial components ("malarial toxins") that activate phagocytes to drive inflammation resulting in systemic symptoms including fever, headaches and rigors. The molecular mechanisms involved in sensing malarial products are poorly understood.

Much progress has been made in our understanding of how phagocytes sense microbial products. In the case of protozoan parasites, the toll-like receptor (TLR) family have been linked to their recognition (Gazzinelli et al., 2004). In humans, polymorphisms in TLR2, 4, 9 and Mal (also known as TIRAP) have been linked to the clinical outcome of malaria (Hawn et al., 2006; Khor et al., 2007; Mockenhaupt et al., 2006). *Plasmodium* glycosylphosphatidylinositol (GPI) anchors trigger TLR2 (Zhu et al., 2005), however, GPI anchors alone cannot account for the immune stimulatory activity of malaria (Wu et al., 2010). Infected erythrocytes contain both the parasite and malaria-derived debris. During the intraerythrocytic stage, parasites digest hemoglobin and produce an inert, insoluble crystal, known as hemozoin, via a detoxification process. Natural hemozoin is coated with both proteins and plasmodial DNA and triggers TLR9 (Parroche et al., 2007; Wu et al., 2010). The ability of hemozoin-DNA to activate TLR9 is likely due to the delivery of plasmodial genomic DNA via hemozoin to the endosomal compartment. Indeed, CpG-containing DNA oligonucleotides designed from the actual sequences of malaria DNA signal via TLR9 (Parroche et al., 2007). The hemozoin crystal itself has also been shown to activate the NLRP3 inflammasome to regulate IL-1β production (Dostert et al., 2009; Griffith et al., 2009; Shio et al., 2009). Mice-deficient in MyD88 and IL1R-IL18R signaling have decreased production of IL-12 and attenuated pathology during infection with murine *Plasmodium spp.* (Adachi et al., 2001; Franklin et al., 2007; Pichyangkul et al., 2004). Studies of cerebral malaria in mice lacking TLRs have suggested that although TLRs contribute to experimental cerebral malaria (ECM), additional mechanisms also contribute (Togbe et al., 2007).

Although polymorphisms in interferon-γ (IFN-γ) -receptor loci are well associated with malarial susceptibility (Koch et al., 2002; Naka et al., 2009), evidence has also linked polymorphisms in the type I IFN receptor (*IFNAR1*) (Aucan et al., 2003) to increased survival. A number of reports have revealed the ability of *Plasmodium* to induce type I IFNs (Aucan et al., 2003; Pichyangkul et al., 2004; Vigario et al., 2007). Type I IFNs are typically generated in response to nucleic acids. Although plasmacytoid dendritic cells (pDCs) are a major source during virus infections, many cell types produce these cytokines. In pDCs,

TLR9 may regulate the IFN response to schizonts (Pichyangkul et al., 2004). Several additional nucleic acid sensors have also been implicated in IFN gene regulation, however their role in malaria has not been explored to date.

In this study we investigated the role of TLR-independent DNA sensors in type I IFN production during malaria. RNA profiling of leukocytes from febrile patients with *P. falciparum* malaria demonstrated elevated expression of interferon-inducible genes (ISGs). Although the malaria genome contains several hundred CpG motifs, and plasmodial DNA as well as schizonts have been shown to activate TLR9 (Parroche et al., 2007; Pichyangkul et al., 2004), the genome is ~ 80% AT (Gardner et al., 2002). In this report, we define a very common AT-rich (AT-r) motif in malaria, *i.e.*, ATTTTTAC, which had previously been noted by others to be proinflammatory when isolated from probiotic bacteria (Shimosato et al., 2006). This motif is present over 6000 times in *P. falciparum*, and is also as commonly found in *P. vivax*. We used the genome of *P. falciparum* to design oligonucleotides (ODN) that contain this AT-r motif which were highly immune stimulatory in both human and murine cells. AT-r DNA activated proinflammatory cytokines such as TNF-α and IL-6, but also activated IFN-β gene transcription. We found that AT-r DNA induced type I IFNs via a pathway that was independent of TLRs, DAI, RNA polymerase III and IFI16/p204 but dependent on Stimulator of Interferon Genes (STING) (Ishikawa and Barber, 2008; Zhong et al., 2008), Tank-binding kinase 1 (TBK1) (Fitzgerald et al., 2003; Ishii et al., 2008) and the Interferon Regulatory Factors 3 (IRF3) and IRF7. Moreover, *Plasmodium* infected RBCs also triggered IFN in macrophages via this STING-dependent pathway. Finally, mice lacking *Tbk1*, *Irf3* and *Irf7* as well as the *Ifnar1* were resistant to lethal cerebral malaria. We suggest that this AT-r DNA sensing pathway is important in the innate immune response to *Plasmodial* infection.

RESULTS

P. falciparum induces Interferon Stimulated Genes (ISGs) during malaria infection

We performed global gene expression profiling of human PBMCs harvested from smear positive symptomatic patients infected with *P. falciparum (Pf)*, before and after curative treatment with anti-malarial drugs. Patients were sick with malaria for 1–3 days (and incubating *Pf* for at least an additional week prior to symptoms) and had either a documented fever at the time of enrollment or a history of fever and/or rigors within the 24-hour period proceeding initial study. We chose to study the same patient before and after curative treatment allowing us to measure effects due to malaria that are not compounded by other potential infections associated with non-malaria infected individuals. An analysis of >580 genes induced revealed the presence of a number of ISGs, including *AIM2*, *OAS1*, *IFITM3*, *CARD12* and *IFITMP4* (Der et al., 1998; Sanda et al., 2006) (Fig. 1A). To determine the direct effect of *Pf* on type I IFNs, we stimulated PBMCs with *Pf* infected red blood cells (iRBC). We found a robust induction of IFNβ mRNA. As expected, uninfected RBCs (uRBC) did not induce IFNβ mRNA (Fig. 1B). The induction of IFNβ by iRBC was similar to that elicited by Sendai virus (Fig. 1B) (Rothenfusser et al., 2005). IFNβ was also induced at the protein level (data not shown).

We have previously demonstrated that natural hemozoin presents plasmodial DNA to TLR9 (Parroche et al., 2007). We therefore purified hemozoin and gDNA from *Pf* cultures and examined their ability to induce IFNβ. Examination of the hemozoin by microscopy confirmed that it was free of contaminating iRBC or parasites (data not shown). Cultured hemozoin induced substantial amounts of IFNβ (Fig. 1C) the activity of which was lost upon DNase treatment. Like hemozoin, purified *Pf* genomic DNA (gDNA) strongly stimulated IFNβ when delivered to the cytosol of cells with cationic lipids (Fig. 1C). Imaging studies showed that the hemozoin crystal was phagocytosed by macrophages and was shortly

thereafter found within the lysosomal compartment (Fig. 1D). At longer timepoints the crystal was found localized in the cytosol showing no lysotracker co-localization. This highlights a mechanism by which hemozoin associated cargo such as plasmodial DNA, might access the cytosol. PBMCs incubated with DNA alone in the absence of lipofectamine failed to upregulate IFNβ (data not shown). These data suggest that plasmodial genomic DNA can drive IFNβ upon access to the cytosolic compartment.

Malarial AT-rich DNA activates both NF-κB and IRF–dependent gene transcription

The high AT-rich content of the malarial genome and the presence of the AT-r motif: ATTTTTAC, found >6000 times in *Plasmodium spp.* prompted us to test if this motif was immunostimulatory. The motif is found in nearly the same abundance in *P. vivax*, a species of *Plasmodium* that is not nearly so AT-rich (Supp Table 1). The motif is also found in viruses, bacteria and the human genome, albeit at lower frequencies.

We designed several oligonucleotides (ODN) that contained the AT-r motif (20mers) with sequences derived from the malarial genome (Supp Table 2). Like *Pf* gDNA all 6 of these AT-r motifs activated the IFNβ promoter in HEK293 cells (Fig. 2A and Sup Fig. 1). ODNs designed on the basis of a portion of the genome located on *Pf* chromosome 9 containing 3 AT-r repeats were stimulatory in HEK293 cells or mouse macrophages (Fig. 2A–B). Human PBMC, THP-1, mouse splenocytes, fibroblasts, bone marrow-derived macrophages (BMDM) and splenic DCs also induced IFNβ mRNA and protein in response to the AT-r ODN (Fig 2B–I). AT-r DNA also induced IFNα (data not shown) and NF-κB activation as well as cytokines like TNFα and IL-6 (Fig. 2J–K).

Secondary structure is a critical determinant of AT-r ODN stimulatory activity

We next designed a series of ODN in which the sequences were modified (Supp Fig. 2A–C). Substituting the central TT with AA, so that the motif was now ATTAATAC, had little effect (Fig. 3A and supp Fig. 2A). In analyzing the active ODN using the mFold algorithm, we realized that all of the active ODN had a stem-loop structure. Disruption of the stem-loop structure substantially reduced their activity (Fig. 3B and supp Fig. 2C). We also assessed if single stranded-ness was a determining factor in the activity of the ODNs. When cells were stimulated with double stranded AT-r ODN, we continued to see a robust activation of IFNβ. We also used the 45bp immunostimulatory DNA (ISD) derived from the *Listeria* genome, which was annealed and prepared the same way as dsAT-r stem-loop. Only ds but not ss ISD induced a robust activation of the IFNβ reporter (Fig 3C). Structural predictions suggested that the AT-r stem-loop DNA hybridized to the reverse strand still had secondary structure, which was not seen when ISD was analyzed in a similar manner (Fig. 3C). Collectively these data indicate that the secondary structure of the AT-rODN is the critical determinant for activity.

AT-r ODN uses a Toll-like receptor-independent signaling pathway

The initial reports of AT-rich DNA elements in probiotic bacteria concluded that their activity was via TLR9 (Shimosato et al., 2006). We have previously reported that *Pf* gDNA can signal via TLR9 (Parroche et al., 2007). To define the role of TLR9 in sensing AT-r ODN we took advantage of HEK293 cell lines that either expressed or lacked TLR9. As CpG-DNA does not trigger IFNβ in HEK293-TLR9 cells, NFκB activation was monitored in this case. *Pf* gDNA was transfected using lipofectamine 2000 or DOTAP, which target DNA to the cytosol or endosome, respectively. *Pf* gDNA (which contains both CpG and AT-r stem-loop DNA motifs) activated NFκB when delivered to the endosomal compartment using DOTAP in TLR9 expressing HEK293 cells but not in the parental HEK293 cell line (Supp figure 3). In contrast, *Pf* gDNA activated NFκB in both cell lines when delivered via lipofectamine (Supp figure 3). These data confirm that *Pf* gDNA can

engage TLR9, when delivered to the endosomal compartment, but triggers an alternative response if delivered to the cytoplasm (Supp Fig. 3).

We next tested the ability of AT-r ODN sequences to trigger IFNβ in *Tlr9*$^{-/-}$ cells. *Pf g*DNA and AT-r ODN delivered via lipofectamine induced normal levels of IFNβ mRNA in spleens from *Tlr9*$^{-/-}$ mice (Fig. 4A). Although CpG containing ODN induced modest amounts of type I IFN, this activity was lost in macrophages and splenocytes harvested from *Tlr9*$^{-/-}$ mice (Fig. 4A and data not shown). *Myd88*$^{-/-}$ *Ticam1*$^{-/-}$ splenocytes and macrophages also responded normally to the presence of cytosolically administered AT-r ODN and *Pf g*DNA ruling out the role of any of the TLRs (Fig. 4B and data not shown).

AT-r stem-loop DNA does not result in the activation of any known nucleic acid sensor

A growing number of nucleotide receptors have been identified which includes Retinoic Inducible Gene-I (RIG-I; encoded by *Ddx58*), Melanoma Differentiation Associated gene-5 (Mda-5; encoded by *Ifih1*)(Kawai et al., 2005; Yoneyama and Fujita, 2009), NOD2 (Sabbah et al., 2009) and DNA-dependent activator of IFN-regulatory factors (DAI; encoded by *Zbp1*) (Takaoka et al., 2007). To examine the role of these sensors, we tested bone marrow cells that were deficient in each of these pathways. *Ifih1*$^{-/-}$, *Ddx58*$^{-/-}$ as well as *Mavs*$^{-/-}$ responded normally to AT-r stem-loop DNA (Fig. 4C–E). Similar results were observed with Nod2$^{-/-}$ and Dai$^{-/-}$ cells (Fig. 4F–G). The reduction of DAI expression in HEK293 cells by RNA interference also had no effect on AT-r ODN activity (Fig. 4H).

AT-r stem-loop DNA uses a distinct pathway from B-form double stranded poly(dA-dT) to induce type I IFNs

In human cells, poly(dA-dT) drives type I IFNs via RNA polymerase III, which converts poly(dA-dT) into a ligand for the RIG-I-MAVS pathway (Ablasser et al., 2009; Chiu et al., 2009). This pathway is redundant with additional sensors in mouse macrophages. To test this pathway, RIG-I, MAVS and RNA polymerase III component 1 (RPC1) were silenced by RNAi in HEK293 cells and IFNβ reporter gene activity measured. siRNA mediated silencing of these components had no effect on the ability of AT-r stem-loop DNA to induce IFNβ gene transcription (Fig. 5A and Sup Fig. 4A). siRNA mediated silencing of these components had no effect on the ability of AT-r stem-loop DNA to induce IFNβ gene transcription. We also tested if transfected AT-r ODN would result in the RNA pol III-dependent production of stimulatory RNA. RNA extracted from transfected 293 cells was tested for its ability to activate RIG-I in PBMCs. Although IFNα was induced with small and total RNA from the poly(dA-dT) transfected cells, *Plasmodial* AT-r stem-loop DNA did not yield a stimulatory RNA (Fig. 5B). Similarly, HEK293 cells were able to induce the activation of the IFNβ reporter in response to RNA extracted from poly(dA-dT) transfected but not in response to AT-r stem-loop DNA derived RNA (Supp Fig. 4B).

We also tested ML-60218, an inhibitor of RNA pol III (Ablasser et al., 2009; Chiu et al., 2009) and NS3/4A (a protease component of the Hepatitis C virus that blocks RIG-I signaling (Foy et al., 2005; Meylan et al., 2005), neither of which had any effect on AT-r ODN induced activation (Fig. 5C and D). Finally, DAI-deficient macrophages treated with the RNA pol III inhibitor ML60218 (Fig. 5E) responded normally, excluding the possibility that DAI and RNA pol III function redundantly. We confirmed these findings in HEK293 cells transfected with DAI-specific shRNA pretreated with ML60218 (Fig 5F). Recently, IFI16 was identified as a sensor of viral DNA that couples to the STING pathway (Unterholzner et al., 2010). siRNA-mediated knockdown of p204 (the murine orthologue of IFI16) prevented HSV and VACV DNA driven IFNβ induction (Fig 5G) but had no effect on AT-r stem-loop DNA (Fig 5G). Knockdown of IFI16 in THP1 cells also failed to affect

AT-r ODN signaling (data not shown). Collectively, these data suggest that AT-r DNA induce IFNβ independently of all currently described DNA sensing receptors.

IFN induction by AT-r stem-loop DNA requires STING, TBK1 and IRF3/7

All cytosolic DNA-induced IFN signaling pathways converge on STING (encoded by *Tmem173*) (Ishikawa and Barber, 2008; Ishikawa et al., 2009; Saitoh et al., 2009) and TBK1 (Fitzgerald et al., 2003; Ishii et al., 2008). Tmem173$^{-/-}$ cells were unable to induce IFNβ in response to AT-r stem-loop DNA or *Pf* gDNA stimulation (Fig. 6A). These findings were corroborated with IFNβ reporter assays in HEK293 cells transfected with STING siRNA (Fig. 6B). STING deficiency also impairs the induction of a number of additional ISGs as well as NF-κB dependent cytokines such as TNFα, IL-6 and IL-15, upon treatment with either AT-rODN or *Pf* genomic DNA (Fig. 6C and Supp. Fig 6). Although *Tbk1*$^{-/-}$ mice die during embryogenesis, this lethality is rescued by crossing these mice to the *Tnfr1*$^{-/-}$ mice (Bonnard et al., 2000). We therefore also compared *Tnfr1*$^{-/-}$ and *Tbk1*$^{-/-}$ *Tnfr1*$^{-/-}$ splenocytes and BMDMs for AT-r ODN-induced IFNβ gene transcription and secretion. *Tbk1*$^{-/-}$ *Tnfr1*$^{-/-}$ splenocytes had a markedly reduced IFNβ response upon challenge with AT-r ODN (Fig. 6D).

We also labeled AT-2 or AT-5 ODN with biotin, and performed streptavidin pull-down assays in lysates from HEK293 cells to examine STING-TBK1 complex formation. The labeled ODN precipitated the STING-TBK1 complex, while a control non-stimulatory ODN, in which the DNA sequences were scrambled failed to immunoprecipitate this complex (Fig. 6E). The immunoprecipitation of STING appears to be dependent on Tbk1, as AT-r ODN precipitated STING in macrophage lysates from *Tnfr1*$^{-/-}$ mice but the same ODN failed to pull down STING from lysates of *Tbk1*$^{-/-}$ *Tnfr1*$^{-/-}$ mice. Moreover, TBK1 was brought down in a complex with the AT-r ODN in *Tmem173*$^{+/+}$ macrophages but failed to do so in *Tmem173*$^{-/-}$ macrophages. Thus, STING and TBK1 associate in this AT-r stem-loop DNA sensing pathway. There is also a partial role for the TBK-1 related kinase IKKε in AT-r stem-loop DNA dependent IFNβ production (Supp Fig. 5A).

The transcriptional enhancer of the IFNβ gene contains contains binding sites for NF-κB; the IRFs (IRF3 and 7) and the heterodimeric complex ATF-2/c- Jun (Panne et al., 2007). AT-r ODN induced reporter gene expression from both the full-length promoter, as well as from reporter genes driven by multimerized individual promoter elements (Fig. 6F and data not shown). Activation of IRF3-IRF7 has been considered a defining event in the transcriptional regulation of the IFNβ gene (Honda and Taniguchi, 2006). IFNβ induction was severely abrogated in splenocytes from *Irf3*$^{-/-}$-*Irf7*$^{-/-}$ DKO mice well as from the single KOs after treatment with AT-rich ODN (Fig. 6G–I). This result suggests that AT-r stem-loop DNA from *Plasmodium* most likely activates type I IFN induction via IRF3 and IRF7 heterodimers. IRF1 and IRF5 were dispensable for ATR-ODN mediated IFNβ induction (Supp Fig. 5B–C).

To examine the physiological relevance of this pathway to malaria infection we conducted a series of *ex vivo* experiments where parasitized RBCs *(P. berghei ANKA* infected RBCs (*PbA* iRBCs) or *Pf* iRBCs) were incubated with mouse macrophages from either wild-type mice or mice deficient in key components of the cytosolic AT-r pathway identified above. Macrophages from *Irf3*$^{-/-}$ *Irf7*$^{-/-}$ or *Tbk1*$^{-/-}$ *Tnfr1*$^{-/-}$ mice failed to induce IFNβ in response to purified *Pf* iRBCs. A similar defect was seen when *PbA* iRBCs were introduced to *Tbk1*$^{-/-}$ *Tnfr1*$^{-/-}$ *or Irf3*$^{-/-}$ *Irf7*$^{-/-}$ cells (Figure 7B–C). We also compared wild type and *Tmem173*$^{-/-}$ cells and as seen in figure 7D, STING-deficiency led to a partial but significant defect in type I IFN responses in response to *PbA* iRBCs.

TBK1-IRF dependent Type I interferon pathway is central to the pathogenesis of experimental cerebral malaria

We next wanted to test if this pathway was important in plasmodial infection *in vivo*. *P. bergheii* ANKA (*PbA*) causes cerebral malarial disease in mice. The model reflects many of the signs of human cerebral malaria, including lethargy, limb paresis-paralysis, vestibular dysfunction, coma and death and is a useful model to assess the contribution of host-factors in the pathogenesis of malaria (Neill and Hunt, 1992). Susceptible strains of mice, when infected with blood stage forms of *P. bergheii* ANKA, rapidly develop parasitemia, cerebral malaria symptoms and typically die within 7–12 days. As seen from our initial analysis of the *Pb*A genome (supplementary Table1), much like *P. falciparum*, *Pb*A is very AT-rich (76%) with a large number of AT-r motifs (~5266). In order to define the role of type I IFNs in this model, wild type mice and *Ifnar1*$^{-/-}$ mice were infected with 1×10^5 parasites of the *PbA*. Parasite loads, survival and development of neurological symptoms typically associated with cerebral progression were monitored over a 22-day period. No differences in parasitemia were observed in the two strains of mice up to the time of death (data not shown). Of the 27 wild-type animals infected, all were dead by day 12; in all but one of these animals, we observed gross neurological abnormalities. In contrast, of the 22 *Ifnar1*$^{-/-}$ tested, only one died on day 19 of parasitemia-induced anemia (Fig. 7E). This difference in outcome was highly statistically significant ($p<0.0001$). Furthermore, *PbA* infections in *Irf3*$^{-/-}$-*Irf7*$^{-/-}$ mice also revealed that these transcription factors are necessary for the progression of cerebral malaria in mouse models, as mice deficient for these factors survived longer than the wildtype mice (Fig. 7F). Similar observations were made when TBK1 hypomorphic mice (TBK1Δ/Δ), as described previously (Marchlik et al.), were used (Fig. 7G). These data indicate that the TBK1-IRF3-IRF7 dependent production of type I IFN and subsequent IFN signaling play an important role in the pathogenesis of cerebral malaria.

DISCUSSION

As all organisms are defined by their nucleic acids, it should not be surprising that nucleic acids have emerged as key triggers of innate immunity. In this report, we have identified a novel DNA sensing pathway important in innate immunity to Malaria. This pathway does not involve any of the known DNA receptors described to date but otherwise follows a canonical core STING-TBK1-IRF signaling pathway. Plasmodial DNA activates this novel AT-r stem-loop DNA sensing pathway either as single stranded or double stranded in a sequence specific manner.

It is probable that AT-r stem-loop DNA only activates this STING-dependent pathway when it finds its way into the cytosol. Experimentally, this was achieved using a transfection reagent like lipofectamine. Our previously published findings, that *plasmodial* DNA signals in DCs via TLR9, were explored using DOTAP (Parroche et al., 2007), a transfection reagent that preferentially targets DNA to the endolysosomal compartment. In the absence of transfection reagents, a key question is how DNA could gain access to cytosolic sensors during an actual infection. We propose that hemozoin acts as a vehicle to deliver DNA to a subcellular compartment where it can have biological effects. This may be particularly relevant as during *Plasmodium* infections, concentrations achieved by free hemozoin in the blood approach 0.2–1mg/ml (Hanscheid et al., 2007). Upon uptake into an immune cell, hemozoin traffics to the phagolysosomal compartment, and TLR9 appears to gain access there to the CpG motifs on the crystalline surface (Parroche et al., 2007). The hemozoin crystal itself activates the cytosolic NLRP3 inflammasome(Dostert et al., 2009; Griffith et al., 2009; Shio et al., 2009). One of the mechanisms by which NLRP3 is activated by crystals like hemozoin, silica and uric acid is a result of their ability to destabilize the phagolysosome, which allows the delivery of phagosomal contents, including cathepsins, to the cytosol (Halle et al., 2008; Hornung et al., 2008). Phagosomal destabilization likely

delivers the AT-r stem-loop DNA into the cytosol, where it could then interact with its cytosolic sensor. Indeed, we have observed that hemozoin causes phagolysosomal instability and allows the contents of this compartment, such as the hemozoin crystal and potentially *P. falciparum* DNA on its crystalline surface, access to the cytosol. These observations suggest that after the uptake of DNA-coated hemozoin, sequential activation of a TLR9-dependent response in the phagolysosome and a TLR9-independent response in the cytosol are likely to occur. This observation is supported by the fact that components of both the TLR9 pathway (namely MyD88) as well as those of the STING-dependent DNA response contribute to the IFN response to parasite laden RBCs. While the defect in *Sting*-deficient cells was incomplete we found a complete defect in type I IFN induction in *Tbk1*$^{-/-}$ *1* and *Irf3*$^{-/-}$ *Irf7*$^{-/-}$ macrophages. Moreover, in line with its previous role in conferring TLR-independent sensitivity to DNA vaccines (Ishii et al., 2008), TBK1 is critical in the development of ECM, likely through the induction of TLR-independent pathways. Thus, our study suggests that two innate pathways are initiated during malaria: a TLR9- and a STING-driven pathway, both of which converge on the IRFs to regulate IFN gene transcription.

A number of reports have revealed the ability of *Plasmodium spp* to induce type I IFNs and a type I IFN gene signature ((Aucan et al., 2003; Pichyangkul et al., 2004; Vigario et al., 2007; Voisine et al.). Previous reports have shown that exogenous recombinant IFNα can even inhibit ECM and reduce parasite burden in mice infected with *P. berghei* ANKA (*PbA*) (Vigario et al., 2007), although this effect requires pretreatment and is reminiscent of the ability of LPS, for example, to prevent Gram-negative sepsis in mice.

Although, pDCs are typically considered major sources of IFNα during microbial infections, recent studies indicate that pDCs are not important in regulating immunity to *P. chaubadi* and *PbA* infections (deWalick et al., 2007; Voisine et al.). In the case of *P. chaubadi*, this observation is not surprising because these mice also do not benefit from the loss of the type I IFN receptor (Voisine et al.). But in mice infected with *PbA*, this is a surprise, given the central role pDCs have in generating type I IFNs. Thus, alternative sources of IFNβ, likely mediated by cells other than pDCs via the cytosolic AT-r ODN pathway may account for the apparent pathology mediated by the type I IFNs in cerebral malaria thus explaining the lack of importance of pDCs in ECM models and perhaps in human cerebral malaria.

The importance of DNA recognition and type I interferon production is only now beginning to be appreciated in a large spectrum of infectious illnesses well beyond the traditional role of IFNα/β in anti-viral immunity. The data in this paper are suggestive that plasmodial DNA has the capability of generating type I IFN (as well as pro-inflammatory cytokines), which in turn determine the outcome of disease. This view of the pathophysiology of malaria is in agreement with the effect of polymorphisms in the human IFN receptors on clinical infections (Aucan et al., 2003; Koch et al., 2002; Naka et al., 2009) as well as by our observation that patients with malaria express a panoply of interferon-stimulated genes. A further observation is that by our analysis, *P. vivax*, although seldom fatal, has a preponderance of both AT-motifs (~5500) as well as CpG motifs (~3000) (data not shown). In contrast, *Pf*, most often associated with fatal malaria, has a rather large number of AT-motifs (~6000) but much smaller numbers of CpG motifs (~300) (data not shown). The importance of this distribution is not immediately clear and may further shift our perception of DNA as a pathogen associated molecular pattern (PAMP) useful in resolving disease.

In view of these results, as well as the emerging literature on DNA sensing, we predict that immune recognition of DNA will be an increasingly common theme in pathogenesis. Microbes as diverse as *Listeria monocytogenes* (O'Connell et al., 2004; Rayamajhi et al.), *Staphylococcus aureus* (Martin et al., 2009), Group B streptococcus (*Streptococcus agalactiae*) (Charrel-Dennis M, 2008) (Xiao et al., 2009) and *Trypanosoma cruzi* (Chessler

et al., 2008) all seem to induce significant amounts of type I IFN through nucleotide recognition. This then suggests that any immunomodulatory therapy contemplated for use as an adjunct for any infectious disease will need to take into account the role of DNA-induced type I IFN in a specific disease and whether or not type I IFNs promote a healthy outcome or enhance pathogenesis.

Experimental Procedures

Mice

Tlr9$^{-/-}$, *Myd88*$^{-/-}$ and *Ticam1*$^{-/-}$ mice (gift of Shizuo Akira, Osaka, Japan) were used to generate *Myd88*$^{-/-}$-*Ticam1*$^{-/-}$ mice. *Dai*$^{-/-}$ and *Irf3*$^{-/-}$-*Irf7*$^{-/-}$ mice were generated from *Irf3*$^{-/-}$ and *Irf7*$^{-/-}$ (gift of Tadagatsu Taniguchi, Tokyo, Japan). *Tbk1*$^{-/+}$ mice from W.C. Yeh (University of Toronto, Ontario, Canada) and were bred with *Tnfr1*$^{-/-}$ mice to generate a double KO. TBK1Δ/Δ micewerefrom Pfizer Pharmaceuticals (MA) (Marchlik et al.). *Ddx58*$^{-/-}$ mice were from S. Akira. *Ifih1*$^{-/-}$ mice were from M. Colonna (Washington University, St. Louis, MI). *Mavs*$^{-/-}$ mice were from of Z.J. Chen (South Western Medical School, Dallas, TX), while *Tmem173*$^{-/-}$ mice were from G. Barber. C57BL/6, *Irf1*$^{-/-}$ and *Irf5*$^{-/-}$ mice were from Jackson Laboratories (Bar Harbor, ME). *Ikkε*$^{-/-}$-deficient mice were from Millenium Pharmaceuticals (Cambridge, MA). All mouse strains were bred and maintained under specific pathogen-free conditions in the animal facilities at the UMass Medical School in accordance with the Institutional Animal Care and Use Committee.

Reagents

CpG 2007 and 1826 were from Coley Pharmaceuticals, (Wellesley, MA). DOTAP was from Roche (Indianapolis, IN) and Lipofectamine 2000 was from Invitrogen (Carlsbad, CA). Poly(dAdT)•Poly(dAdT) and poly(I:C) were from Sigma-Aldrich and Imigenex, respectively. Lysotracker was from Molecular probes/Invitrogen (Carlsbad, CA). Forward and reverse strands of Interferon Stimulating DNA (Stetson and Medzhitov, 2006) were obtained from IDT (Coralville, IA). *Pf* 3D7 gDNA was obtained from the Malaria research and reference reagent resource center (MR4) at NIAID. Human embryonic kidney 293 cells were obtained from ATCC (Manassas, VA). ML60218 was from Calbiochem.

Cell culture, stimulation and microscopy

Mouse bone marrow–derived macrophages, human PBMCs, primary cells, HEK293, and THP-1s were cultured as described (Hornung et al., 2009; Rathinam et al., 2010). Splenocytes and pan-DC subpopulations were isolated from spleens as described (Goutagny et al., 2010). For stimulations, poly(dA-dT) (1 μg/ml), ISD (3μM) and AT-r stem-loop DNA(3μM) was transfected using lipofectamine 2000 according to the manufacturer's instructions. Newcastle Disease Virus (NDV, LaSota strain) was obtained from P. Pitha (Johns Hopkins, Baltimore, MD). Sendai Virus (SeV, Cantrell strain) was from Charles River Laboratories (Wilmington, MA). 1×10^5 macrophages were plated with indicated numbers of Pf or PbA infected RBCs or uninfected RBCs for 48hrs. For immunofluoresence 5×10^5 macrophages in a confocal dish were stimulated with 200μM natural hemozoin for 1 and 6hrs. Lysotracker (Molecular Probes/invitrogen) was added to cells at a final dilution of 1:10000 in media for 15 minutes to visualize the lysosomes. Specifically hemozoin in cells was visualized using acousto-reflection microscopy with a Leica SP2 microscope as described (Hornung et al., 2008).

RNA extraction and real time PCR

Human PBMC, mouse BMDM, HEK293 or mouse splenocytes ($3–10\times10^6$ cells/condition), were stimulated for 6 to 17h using Hemozoin (100μM) or poly(dA-dT) (5μg/ml), CpG

motifs (5μM), AT-rich ODN (3μM), or *Pf* gDNA (5μg) all of which were transfected with lipofectamine 2000 (Invitrogen). RNA was extracted with RNeasy kit (Qiagen, CA), cDNA was synthesized, and quantitative RT-PCR analysis was performed with primers as described (Charrel-Dennis et al., 2008; Goutagny et al., 2010). Gene expression data is presented as a ratio of gene copy number per 100 copies of Actin ± SD.

P. falciparum culture

Erythrocytic stages of *Pf* 3D7 isolates were cultured and natural hemozoin and DNA from *Pf* were purified as described (Parroche et al., 2007). For iRBC preparation, malaria cultures were synchronized with sorbitol for 3 cycles. *Pf* culture stage and parasitemia was assessed daily by field staining. Where indicated, *Pf* enriched cultures at 8% parasitemia and trophozoite or schizont stages were purified as described (Baratin et al., 2005; Cooper et al., 2005; Wu et al., 2010). The culture was then adjusted to a parasitemia of 8% and used to stimulate PBMCs at 40% hematocrit.

P. berghei ANKA induced cerebral malaria model

The *P. berghei ANKA* (Pba) strain (gift of A. Luster, Harvard, Boston, MA) was maintained by passage in C57BL/6 mice. Mice were inoculated i.p. with 1×10^5 infected RBCs and neurological symptoms and death were recorded daily. Cerebral malaria was diagnosed by clinical signs including ataxia, paralysis, deviation of the head, convulsions, and coma, followed by death. Moribund animals were scored as dead, and euthanized. For *ex vivo* infections with PbA iRBCs, BALB/c mice were injected with PbA at 1×10^5 iRBCs and parasitemia was monitored daily. Blood was collected by cardiac puncture at 65% parasitemia.

Design of *P. falciparum* AT-motifs and secondary structure modeling

20 mer AT-ODN containing the consensus motif: 5′-NNNNNNATTTTTACNNNNNN-3′ were identified in the *Pf genome* using Fuzznuc, an algorithm from the EMBOSS package (http://emboss.sourceforge.net/apps/release/6.2/emboss/apps/fuzznuc.html). The Fuzznuc reverse option was enabled so that both DNA strands were screened. All AT-rich ODN, including biotin-labeled ODN, were synthesized by IDT (San Jose, CA) and tested on both phosphodiester (PD) and phosphorothiorate (PS) backbones in different cell types. All AT-r stem-loop DNA sequences were uploaded on mFold (M. Zuker) and secondary structure modeling was carried out at 37°C and default [Mg^{2+}].

Microarray Analysis

Human studies were approved by the University of Massachusetts Medical School Institutional Review Board, the local IRBs of the Brazilian institutions and the Brazilian national IRB (CONEP approval number 10567). Portions of the microarray analysis have been previously reported (Franklin et al., 2009) where the methodology is reported in detail. The data was deposited in NCBIs Gene Expression Omnibus (GEO, http://www.ncbi.nlm.nih.gov/geo/; GSE15221). The current study represents 14 otherwise healthy patients (from Porto Vehlo, Brazil) who were naturally infected with *P. falciparum* before and 3–5 weeks after documented curative treatment with mefloquine. Each patient served as his/her own control. PCR was used to exclude patients with mixed infections involving *P. vivax*. Simple filtering, normalization and averaging were carried out using BASE (Bio-Array Software Environment) (https://base.mgh.harvard.edu/) and log transformed (log2). Genes were filtered to include only genes with a signal greater than the average signal from the negative controls in at least one of the samples with a detection p-value less than 0.01. Differences in gene expression between the two conditions were

considered significant if $p<0.01$ with a paired t test with Benjamini-Hochberg correction for multiple testing and a fold change greater than 1.7.

ELISA

Cell culture supernatants were assayed for huIFNα by ELISA (R&D or Bender MedSystems), according to the manufacturer's instructions. The mouse TNFα and IL-6 kits were from e-Biosciences, while the murine IFNβ kit is as described (Roberts et al., 2007).

Reporter assays

(2×10^4 cells/well) HEK293, were plated in 96 well plates and stimulated for 24h as outlined above and IFNβ, PRDIII-I, PPRD-II, PRD-IV and NF-kB luciferase reporter activity measured as described (Rothenfusser et al., 2005). The full length IFNβ promoter, PRDIII-I, PRDII and PRDIV luciferase reporters were from T. Maniatis (Harvard University, Boston, MA). pGL4-TK Renilla luciferase and pGL3-control luciferase were from Promega (Madison, WI). pME18-NS3/4A-myc and NS3/4S139A-myc were from Z.J. Chen (UT Southwestern, Dallas, Texas). The pGL3-enhancer-ELAM-minimal promoter was used to assess NF-κB activity.

RNA preparation and Nanostring experiment

If not indicated otherwise, DNA-transfected or SeV-infected 293 cells (2.4×10^5 cells per 12 wells) were collected 9h or 18h after stimulation. The Mini RNA Isolation II kit (Zymo Research) was used for RNA isolation with the previously described modifications (Ablasser et al., 2009). nCounter CodeSets were constructed to detect selected mouse-specific genes as described previously (Dixit et al.). 2×10^5 BMDMs from *Tmem173*+/+ and *Tmem173*−/− animals were lysed in RLT buffer (QIAGEN) supplemented with β-mercaptoethanol. Five percent of this lysate (containing 10^4 cells) was hybridized to the Codeset for 16hr and loaded onto the nCounter prep station, followed by quantification with the nCounter Digital Analyzer. For side-by-side comparisons of nCounter experiments, data was normalized in two ways described previously (Dixit et al.).

RNA-mediated interference

First, siRNA was reverse-transfected at a concentration of 25nM into $TLR3^+$-HEK293 cells (4×10^4 cells per 96 wells) with 0.5 μl lipofectamine. 48 h after transfection, cells were stimulated and after an additional period of 24 h levels of IFNβ mRNA were assessed using RT-PCR. Poly(I:C) was added at 100 ng/ml final concentration, while transfected poly(I:C) was introduced at 10ng/ml. siRNA sequences used for RNA-polymerase III, MAVS, RIG-I and STING were obtained from Qiagen or Invitrogen and are as described (Ablasser et al., 2009) (Ishikawa and Barber, 2008).

Pulldown assays and Immunoblotting

3×10^6 HEK293s or *Tmem173*$^{-/-}$, *Tmem173*$^{+/+}$, *Tbk1*$^{-/-}$ *Tnfr1*$^{-/-}$ and *Tnfr1*$^{-/-}$ BMDM were lysed with lysis buffer containing NP-40, dithiothreitol (DTT), phenylmethylsulfonyl fluoride (PMSF) and sodium orthovanadate (Na_3VO_4) for 20 min at 4°C. Lysates were spun to remove debris and then incubated with 1μg of 3′ or 5′-biotinylated AT2 (PS) or AT5 (PD) and streptavidin-agarose beads (50% w/v) for 2 hours. Lysates were spun to obtain the bead pellet, washed and boiled with loading buffer containing SDS and run on 10% SDS-polyacrylamide gel. Blots were probed using the STING antibody as described (Ishikawa and Barber, 2008), anti-TBK1 was obtained from Imgenex and anti-β-actin was from Sigma.

ShRNA mediated silencing

The lentiviral shRNA sequences were cloned into pLKO.1 TRC cloning vector 56. The silencing sequence was from the MISSION™ TRC-Hs 1.0 (Human) as follows: TRCN0000-123051 for DAI. The production of viral particles and transduction of target cells were conducted according to the following protocols (http://www.broad.mit.edu/genome_bio/trc/publicProtocols.html). Knockdown efficiency was assessed by one step RT-PCR (Invitrogen) using the following primers: DAI-F ATCTGCCTGGAGTTACCTTC; DAI-R TCTGGATTTCCTGACCTATTG and antibody to DAI (Imgenex).

Statistical analysis

Differences between groups were analyzed for statistical significance by using Student's t-test. $P < 0.05$ was considered as statistically significant.

Supplementary Material

Refer to Web version on PubMed Central for supplementary material.

Acknowledgments

The authors would like to thank A. Cerny for animal husbandry and genotyping and O. Mulhern for her help with affinity purification assays. This work is supported by NIH grants AI067497 (to K.A.F), by AI079293 (to K.A.F and D.T.G) and by R21AI80907 (to R.T.G).

References

Ablasser A, Bauernfeind F, Hartmann G, Latz E, Fitzgerald K, Hornung V. RIG-I-dependent sensing of poly(dA:dT) through the induction of an RNA polymerase III-transcribed RNA intermediate. Nat Immunol. 2009

Adachi K, Tsutsui H, Kashiwamura S, Seki E, Nakano H, Takeuchi O, Takeda K, Okumura K, Van Kaer L, Okamura H, et al. Plasmodium berghei infection in mice induces liver injury by an IL-12- and toll-like receptor/myeloid differentiation factor 88-dependent mechanism. J Immunol. 2001; 167:5928–5934. [PubMed: 11698470]

Aucan C, Walley AJ, Hennig BJ, Fitness J, Frodsham A, Zhang L, Kwiatkowski D, Hill AV. Interferon-alpha receptor-1 (IFNAR1) variants are associated with protection against cerebral malaria in the Gambia. Genes Immun. 2003; 4:275–282. [PubMed: 12761564]

Baratin M, Roetynck S, Lepolard C, Falk C, Sawadogo S, Uematsu S, Akira S, Ryffel B, Tiraby JG, Alexopoulou L, et al. Natural killer cell and macrophage cooperation in MyD88-dependent innate responses to Plasmodium falciparum. Proc Natl Acad Sci U S A. 2005; 102:14747–14752. [PubMed: 16203971]

Bonnard M, Mirtsos C, Suzuki S, Graham K, Huang J, Ng M, Itie A, Wakeham A, Shahinian A, Henzel WJ, et al. Deficiency of T2K leads to apoptotic liver degeneration and impaired NF-kappaB-dependent gene transcription. EMBO J. 2000; 19:4976–4985. [PubMed: 10990461]

Charrel-Dennis M, et al. TLR-independent type I interferon induction in response to an extracellular bacterial pathogen via intracellular recognition of its DNA. Cell Host Microbe. 2008:543–554. [PubMed: 19064255]

Charrel-Dennis M, Latz E, Halmen KA, Trieu-Cuot P, Fitzgerald KA, Kasper DL, Golenbock DT. TLR-independent type I interferon induction in response to an extracellular bacterial pathogen via intracellular recognition of its DNA. Cell Host Microbe. 2008; 4:543–554. [PubMed: 19064255]

Chessler AD, Ferreira LR, Chang TH, Fitzgerald KA, Burleigh BA. A novel IFN regulatory factor 3-dependent pathway activated by trypanosomes triggers IFN-beta in macrophages and fibroblasts. J Immunol. 2008; 181:7917–7924. [PubMed: 19017982]

Chiu Y, Macmillan J, Chen Z. Polymerase III detects cytosolic DNA and induces Type I interferons through the RIG-I pathway. Cell. 2009:576–591. [PubMed: 19631370]

Clark IA, Alleva LM, Mills AC, Cowden WB. Pathogenesis of malaria and clinically similar conditions. Clin Microbiol Rev. 2004; 17:509–539. table of contents. [PubMed: 15258091]

Cooper RA, Papakrivos J, Lane KD, Fujioka H, Lingelbach K, Wellems TE. PfCG2, a Plasmodium falciparum protein peripherally associated with the parasitophorous vacuolar membrane, is expressed in the period of maximum hemoglobin uptake and digestion by trophozoites. Mol Biochem Parasitol. 2005; 144:167–176. [PubMed: 16183150]

Der SD, Zhou A, Williams BR, Silverman RH. Identification of genes differentially regulated by interferon alpha, beta, or gamma using oligonucleotide arrays. Proc Natl Acad Sci U S A. 1998; 95:15623–15628. [PubMed: 9861020]

deWalick S, Amante FH, McSweeney KA, Randall LM, Stanley AC, Haque A, Kuns RD, MacDonald KP, Hill GR, Engwerda CR. Cutting edge: conventional dendritic cells are the critical APC required for the induction of experimental cerebral malaria. J Immunol. 2007; 178:6033–6037. [PubMed: 17475826]

Dixit E, Boulant S, Zhang Y, Lee AS, Odendall C, Shum B, Hacohen N, Chen ZJ, Whelan SP, Fransen M, et al. Peroxisomes are signaling platforms for antiviral innate immunity. Cell. 141:668–681. [PubMed: 20451243]

Dostert C, Guarda G, Romero JF, Menu P, Gross O, Tardivel A, Suva ML, Stehle JC, Kopf M, Stamenkovic I, et al. Malarial hemozoin is a Nalp3 inflammasome activating danger signal. PLoS One. 2009; 4:e6510. [PubMed: 19652710]

Fitzgerald KA, McWhirter SM, Faia KL, Rowe DC, Latz E, Golenbock DT, Coyle AJ, Liao SM, Maniatis T. IKKepsilon and TBK1 are essential components of the IRF3 signaling pathway. Nat Immunol. 2003; 4:491–496. [PubMed: 12692549]

Foy E, Li K, Sumpter R Jr, Loo YM, Johnson CL, Wang C, Fish PM, Yoneyama M, Fujita T, Lemon SM, Gale M Jr. Control of antiviral defenses through hepatitis C virus disruption of retinoic acid-inducible gene-I signaling. Proc Natl Acad Sci U S A. 2005; 102:2986–2991. [PubMed: 15710892]

Franklin BS, Parroche P, Ataide MA, Lauw F, Ropert C, de Oliveira RB, Pereira D, Tada MS, Nogueira P, da Silva LH, et al. Malaria primes the innate immune response due to interferon-gamma induced enhancement of toll-like receptor expression and function. Proc Natl Acad Sci U S A. 2009; 106:5789–5794. [PubMed: 19297619]

Franklin BS, Rodrigues SO, Antonelli LR, Oliveira RV, Goncalves AM, Sales-Junior PA, Valente EP, Alvarez-Leite JI, Ropert C, Golenbock DT, Gazzinelli RT. MyD88-dependent activation of dendritic cells and CD4(+) T lymphocytes mediates symptoms, but is not required for the immunological control of parasites during rodent malaria. Microbes Infect. 2007; 9:881–890. [PubMed: 17537666]

Gardner MJ, Hall N, Fung E, White O, Berriman M, Hyman RW, Carlton JM, Pain A, Nelson KE, Bowman S, et al. Genome sequence of the human malaria parasite Plasmodium falciparum. Nature. 2002; 419:498–511. [PubMed: 12368864]

Gazzinelli RT, Ropert C, Campos MA. Role of the Toll/interleukin-1 receptor signaling pathway in host resistance and pathogenesis during infection with protozoan parasites. Immunol Rev. 2004; 201:9–25. [PubMed: 15361229]

Goutagny N, Jiang Z, Tian J, Parroche P, Schickli J, Monks BG, Ulbrandt N, Ji H, Kiener PA, Coyle AJ, Fitzgerald KA. Cell type-specific recognition of human metapneumoviruses (HMPVs) by retinoic acid-inducible gene I (RIG-I) and TLR7 and viral interference of RIG-I ligand recognition by HMPV-B1 phosphoprotein. J Immunol. 2010; 184:1168–1179. [PubMed: 20042593]

Griffith JW, Sun T, McIntosh MT, Bucala R. Pure Hemozoin is inflammatory in vivo and activates the NALP3 inflammasome via release of uric acid. J Immunol. 2009; 183:5208–5220. [PubMed: 19783673]

Halle A, Hornung V, Petzold GC, Stewart CR, Monks BG, Reinheckel T, Fitzgerald KA, Latz E, Moore KJ, Golenbock DT. The NALP3 inflammasome is involved in the innate immune response to amyloid-beta. Nat Immunol. 2008; 9:857–865. [PubMed: 18604209]

Hanscheid T, Egan TJ, Grobusch MP. Haemozoin: from melatonin pigment to drug target, diagnostic tool, and immune modulator. Lancet Infect Dis. 2007; 7:675–685. [PubMed: 17897610]

Hawn TR, Dunstan SJ, Thwaites GE, Simmons CP, Thuong NT, Lan NT, Quy HT, Chau TT, Hieu NT, Rodrigues S, et al. A polymorphism in Toll-interleukin 1 receptor domain containing adaptor protein is associated with susceptibility to meningeal tuberculosis. J Infect Dis. 2006; 194:1127–1134. [PubMed: 16991088]

Honda K, Taniguchi T. IRFs: master regulators of signalling by Toll-like receptors and cytosolic pattern-recognition receptors. Nat Rev Immunol. 2006; 6:644–658. [PubMed: 16932750]

Hornung V, Ablasser A, Charrel-Dennis M, Bauernfeind F, Horvath G, et al. AIM2 recognizes cytosolic dsDNA and forms a caspase-1-activating inflammasome with ASC. Nature. 2009

Hornung V, Bauernfeind F, Halle A, Samstad EO, Kono H, Rock KL, Fitzgerald KA, Latz E. Silica crystals and aluminum salts activate the NALP3 inflammasome through phagosomal destabilization. Nat Immunol. 2008; 9:847–856. [PubMed: 18604214]

Ishii KJ, Kawagoe T, Koyama S, Matsui K, Kumar H, Kawai T, Uematsu S, Takeuchi O, Takeshita F, Coban C, Akira S. TANK-binding kinase-1 delineates innate and adaptive immune responses to DNA vaccines. Nature. 2008; 451:725–729. [PubMed: 18256672]

Ishikawa H, Barber GN. STING is an endoplasmic reticulum adaptor that facilitates innate immune signalling. Nature. 2008; 455:674–678. [PubMed: 18724357]

Ishikawa H, Ma Z, Barber GN. STING regulates intracellular DNA-mediated, type I interferon-dependent innate immunity. Nature. 2009:1–5.

Kawai T, Takahashi K, Sato S, Coban C, Kumar H, Kato H, Ishii KJ, Takeuchi O, Akira S. IPS-1, an adaptor triggering RIG-I- and Mda5-mediated type I interferon induction. Nat Immunol. 2005; 6:981–988. [PubMed: 16127453]

Khor CC, Chapman SJ, Vannberg FO, Dunne A, Murphy C, Ling EY, Frodsham AJ, Walley AJ, Kyrieleis O, Khan A, et al. A Mal functional variant is associated with protection against invasive pneumococcal disease, bacteremia, malaria and tuberculosis. Nat Genet. 2007; 39:523–528. [PubMed: 17322885]

Koch O, Awomoyi A, Usen S, Jallow M, Richardson A, Hull J, Pinder M, Newport M, Kwiatkowski D. IFNGR1 gene promoter polymorphisms and susceptibility to cerebral malaria. J Infect Dis. 2002; 185:1684–1687. [PubMed: 12023780]

Marchlik E, Thakker P, Carlson T, Jiang Z, Ryan M, Marusic S, Goutagny N, Kuang W, Askew GR, Roberts V, et al. Mice lacking Tbk1 activity exhibit immune cell infiltrates in multiple tissues and increased susceptibility to LPS-induced lethality. J Leukoc Biol. 88:1171–1180. [PubMed: 20651301]

Martin FJ, Gomez MI, Wetzel DM, Memmi G, O'Seaghdha M, Soong G, Schindler C, Prince A. Staphylococcus aureus activates type I IFN signaling in mice and humans through the Xr repeated sequences of protein A. J Clin Invest. 2009; 119:1931–1939. [PubMed: 19603548]

Meylan E, Curran J, Hofmann K, Moradpour D, Binder M, Bartenschlager R, Tschopp J. Cardif is an adaptor protein in the RIG-I antiviral pathway and is targeted by hepatitis C virus. Nature. 2005

Mockenhaupt FP, Cramer JP, Hamann L, Stegemann MS, Eckert J, Oh NR, Otchwemah RN, Dietz E, Ehrhardt S, Schroder NW, et al. Toll-like receptor (TLR) polymorphisms in African children: Common TLR-4 variants predispose to severe malaria. Proc Natl Acad Sci U S A. 2006; 103:177–182. [PubMed: 16371473]

Naka I, Patarapotikul J, Hananantachai H, Tokunaga K, Tsuchiya N, Ohashi J. IFNGR1 polymorphisms in Thai malaria patients. Infect Genet Evol. 2009; 9:1406–1409. [PubMed: 19712753]

Neill AL, Hunt NH. Pathology of fatal and resolving Plasmodium berghei cerebral malaria in mice. Parasitology. 1992; 105(Pt 2):165–175. [PubMed: 1280805]

O'Connell RM, Saha SK, Vaidya SA, Bruhn KW, Miranda GA, Zarnegar B, Perry AK, Nguyen BO, Lane TF, Taniguchi T, et al. Type I interferon production enhances susceptibility to Listeria monocytogenes infection. J Exp Med. 2004; 200:437–445. [PubMed: 15302901]

Panne D, Maniatis T, Harrison SC. An atomic model of the interferon-beta enhanceosome. Cell. 2007; 129:1111–1123. [PubMed: 17574024]

Parroche P, Lauw FN, Goutagny N, Latz E, Monks BG, Visintin A, Halmen KA, Lamphier M, Olivier M, Bartholomeu DC, et al. Malaria hemozoin is immunologically inert but radically enhances

innate responses by presenting malaria DNA to Toll-like receptor 9. Proc Natl Acad Sci U S A. 2007; 104:1919–1924. [PubMed: 17261807]

Pichyangkul S, Yongvanitchit K, Kum-arb U, Hemmi H, Akira S, Krieg AM, Heppner DG, Stewart VA, Hasegawa H, Looareesuwan S, et al. Malaria blood stage parasites activate human plasmacytoid dendritic cells and murine dendritic cells through a Toll-like receptor 9-dependent pathway. J Immunol. 2004; 172:4926–4933. [PubMed: 15067072]

Rathinam VA, Jiang Z, Waggoner SN, Sharma S, Cole LE, Waggoner L, Vanaja SK, Monks BG, Ganesan S, Latz E, et al. The AIM2 inflammasome is essential for host defense against cytosolic bacteria and DNA viruses. Nat Immunol. 2010; 11:395–402. [PubMed: 20351692]

Rayamajhi M, Humann J, Penheiter K, Andreasen K, Lenz LL. Induction of IFN-alphabeta enables Listeria monocytogenes to suppress macrophage activation by IFN-gamma. J Exp Med. 207:327–337. [PubMed: 20123961]

Roberts ZJ, Goutagny N, Perera PY, Kato H, Kumar H, Kawai T, Akira S, Savan R, van Echo D, Fitzgerald KA, et al. The chemotherapeutic agent DMXAA potently and specifically activates the TBK1-IRF-3 signaling axis. J Exp Med. 2007; 204:1559–1569. [PubMed: 17562815]

Rothenfusser S, Goutagny N, Diperna G, Gong M, Monks BG, Schoenemeyer A, Yamamoto M, Akira S, Fitzgerald KA. The RNA Helicase Lgp2 Inhibits TLR-Independent Sensing of Viral Replication by Retinoic Acid-Inducible Gene-I. J Immunol. 2005; 175:5260–5268. [PubMed: 16210631]

Sabbah A, Chang TH, Harnack R, Frohlich V, Tominaga K, Dube PH, Xiang Y, Bose S. Activation of innate immune antiviral responses by Nod2. Nat Immunol. 2009; 10:1073–1080. [PubMed: 19701189]

Saitoh T, Fujita N, Hayashi T, Takahara K, Satoh T, Lee H, Matsunaga K, Kageyama S, Omori H, Noda T, et al. Atg9a controls dsDNA-driven dynamic translocation of STING and the innate immune response. Proc Natl Acad Sci U S A. 2009

Sanda C, Weitzel P, Tsukahara T, Schaley J, Edenberg HJ, Stephens MA, McClintick JN, Blatt LM, Li L, Brodsky L, Taylor MW. Differential gene induction by type I and type II interferons and their combination. J Interferon Cytokine Res. 2006; 26:462–472. [PubMed: 16800785]

Shimosato T, Kimura T, Tohno M, Iliev ID, Katoh S, Ito Y, Kawai Y, Sasaki T, Saito T, Kitazawa H. Strong immunostimulatory activity of AT-oligodeoxynucleotide requires a six-base loop with a self-stabilized 5′-C…G-3′ stem structure. Cell Microbiol. 2006; 8:485–495. [PubMed: 16469059]

Shio MT, Eisenbarth SC, Savaria M, Vinet AF, Bellemare MJ, Harder KW, Sutterwala FS, Bohle DS, Descoteaux A, Flavell RA, Olivier M. Malarial hemozoin activates the NLRP3 inflammasome through Lyn and Syk kinases. PLoS Pathog. 2009; 5:e1000559. [PubMed: 19696895]

Stetson DB, Medzhitov R. Recognition of cytosolic DNA activates an IRF3-dependent innate immune response. Immunity. 2006; 24:93–103. [PubMed: 16413926]

Takaoka A, Wang Z, Choi MK, Yanai H, Negishi H, Ban T, Lu Y, Miyagishi M, Kodama T, Honda K, et al. DAI (DLM-1/ZBP1) is a cytosolic DNA sensor and an activator of innate immune response. Nature. 2007; 448:501–505. [PubMed: 17618271]

Togbe D, Schofield L, Grau GE, Schnyder B, Boissay V, Charron S, Rose S, Beutler B, Quesniaux VF, Ryffel B. Murine cerebral malaria development is independent of toll-like receptor signaling. Am J Pathol. 2007; 170:1640–1648. [PubMed: 17456769]

Unterholzner L, Keating SE, Baran M, Horan KA, Jensen SB, Sharma S, Sirois C, Jin T, Xiao T, Fitzgerald KA, et al. IFI16 is a novel innate immune sensor for cytoplasmic DNA. Nat Immunol. 2010

Vigario AM, Belnoue E, Gruner AC, Mauduit M, Kayibanda M, Deschemin JC, Marussig M, Snounou G, Mazier D, Gresser I, Renia L. Recombinant human IFN-alpha inhibits cerebral malaria and reduces parasite burden in mice. J Immunol. 2007; 178:6416–6425. [PubMed: 17475871]

Voisine C, Mastelic B, Sponaas AM, Langhorne J. Classical CD11c+ dendritic cells, not plasmacytoid dendritic cells, induce T cell responses to Plasmodium chabaudi malaria. Int J Parasitol. 40:711–719. [PubMed: 19968996]

Wu X, Gowda NM, Kumar S, Gowda DC. Protein-DNA Complex Is the Exclusive Malaria Parasite Component that Activates Dendritic Cells and Triggers Innate Immune Responses. J Immunol. 2010

Xiao N, Eidenschenk C, Krebs P, Brandl K, Blasius AL, Xia Y, Khovananth K, Smart NG, Beutler B. The Tpl2 mutation Sluggish impairs type I IFN production and increases susceptibility to group B streptococcal disease. J Immunol. 2009; 183:7975–7983. [PubMed: 19923465]

Yoneyama M, Fujita T. RNA recognition and signal transduction by RIG-I like receptors. Immunological Reviews. 2009; 227:54–65. [PubMed: 19120475]

Zhong B, Yang Y, Li S, Wang YY, Li Y, Diao F, Lei C, He X, Zhang L, Tien P, Shu HB. The adaptor protein MITA links virus-sensing receptors to IRF3 transcription factor activation. Immunity. 2008; 29:538–550. [PubMed: 18818105]

Zhu J, Krishnegowda G, Gowda DC. Induction of proinflammatory responses in macrophages by the glycosylphosphatidylinositols of Plasmodium falciparum: the requirement of extracellular signal-regulated kinase, p38, c-Jun N-terminal kinase and NF-kappaB pathways for the expression of proinflammatory cytokines and nitric oxide. J Biol Chem. 2005; 280:8617–8627. [PubMed: 15611045]

HIGHLIGHTS

1. *Plasmodium falciparum* induces type I IFN inducible genes during infections.
2. *Pf* genomic DNA is AT-rich and induces type I IFNs in a TLR9-independent manner.
3. *Pf* AT-rich DNA triggers a STING-dependent DNA sensing pathway.
4. Malarial pathology involves TBK1 and IRF3-IRF7-dependent production of type I IFNs.

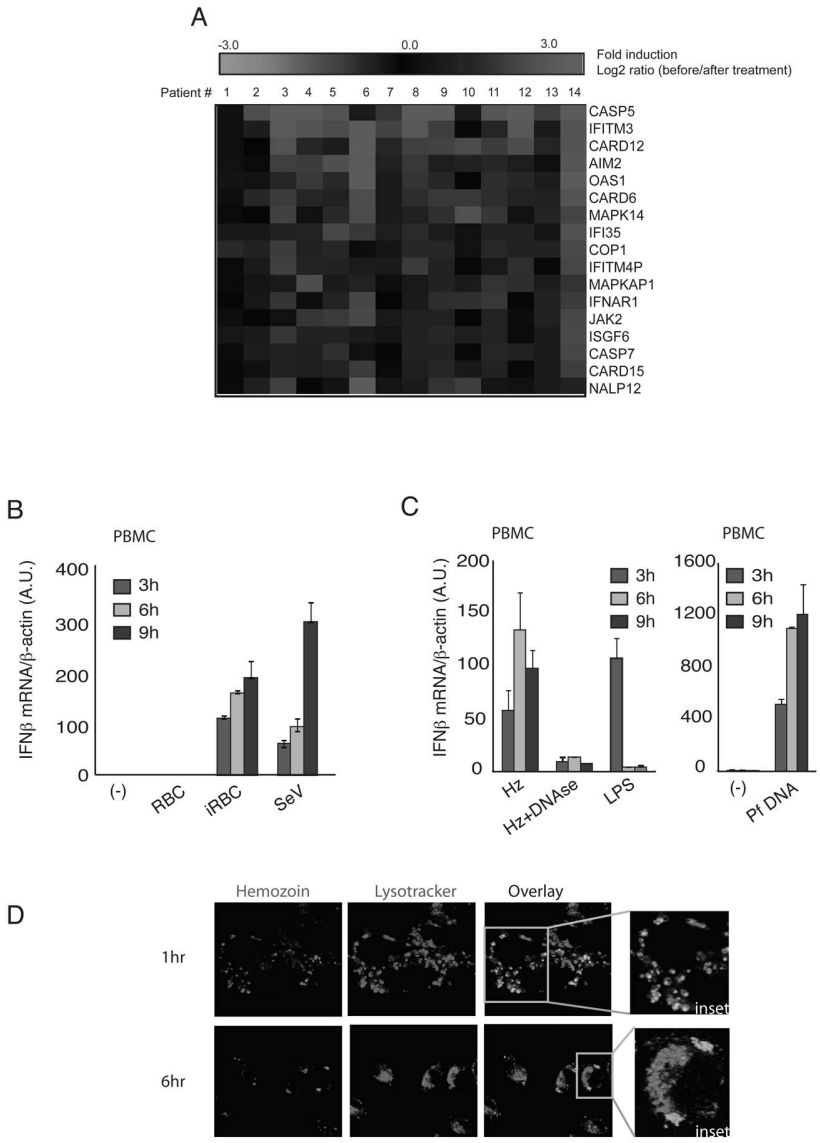

Figure 1. *P. falciparum* induced interferon stimulated gene expression in human cells

A. A microarray analysis of PBMCs from 14 patients infected with *Pf*, before or after curative treatment with mefloquine. A selection of ISGs from a cohort of 580 upregulated genes is depicted. **B.** PBMCs were stimulated with *Pf*-infected red blood cells (iRBC), uninfected RBCs (RBCs) or SeV (200HAU/ml) for 3 to 9 hours. **C.** PBMCs were stimulated with LPS (100ng/ml), 100μM natural hemozoin (Hz) untreated or pretreated with *S. aureus* micrococcal nuclease (Hz + DNAse) or 5 μg of genomic DNA (Pf *g*DNA) complexed with lipofectamine 2000. IFNβ and β-actin mRNA was measured by qPCR. **D.** Mouse BMDM were treated with 200μM Hz and Hz and lysosomes were visualized with acousto-reflection microscopy and lysotracker respectively. Fields are representative of at least 10 fields of view.

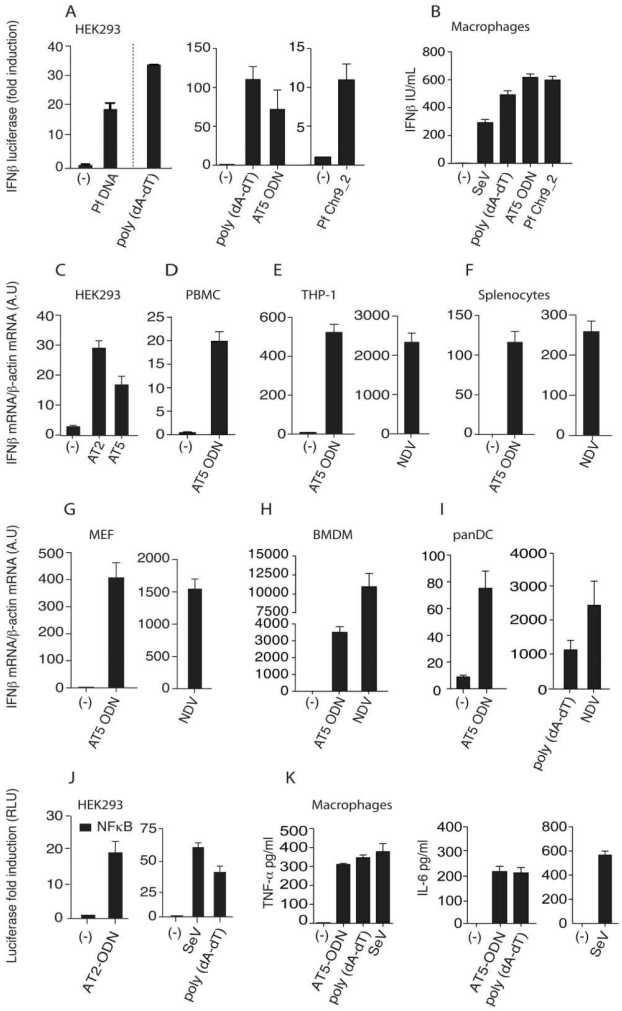

Figure 2. Immune stimulatory activity of AT-rich motifs from *P. falciparum*

A. IFNβ reporter gene activity was measured from cells stimulated with media alone (−), purified *Pf* g DNA (5μg/ml), AT5 rich ODN (20-mer, 3μM, phosphorothiorate backbone (PS)), *Pf* chromosomal-derived Pf Chr 9_2 long ODN (56-mer, 3μM, PS), poly (dA-dT) (5μg/ml) complexed with lipofectamine 2000. Data are represented as fold induction relative to the reporter-only control and reflect mean fold induction ± SD. **B.** BMDM were stimulated with AT-rich ODN on phosphodiester backbones (PD), SeV and pdAdT. IFNβ secretion was measured 16h later by ELISA. **C–I.** HEK293, PBMCs, THP-1, mouse splenocytes, embryonic fibroblasts (MEFs), BMDMs and splenic dendritic cells (panDCs) were stimulated for 6h with 3μM AT2/AT5 (PS) or AT5 (PD) and IFNβ levels measured by qPCR. **J.** NF-κB reporter gene activity in HEK293 cells stimulated with AT2 (3μM, PS), poly (dA-dT) (5μg/ml), or infected with SeV (200HAU/ml). **K.** IL-6 or TNFα levels were measured 18h later by ELISA from macrophages treated as indicated. Data are presented as mean ± SD and are representative of 3 independent experiments.

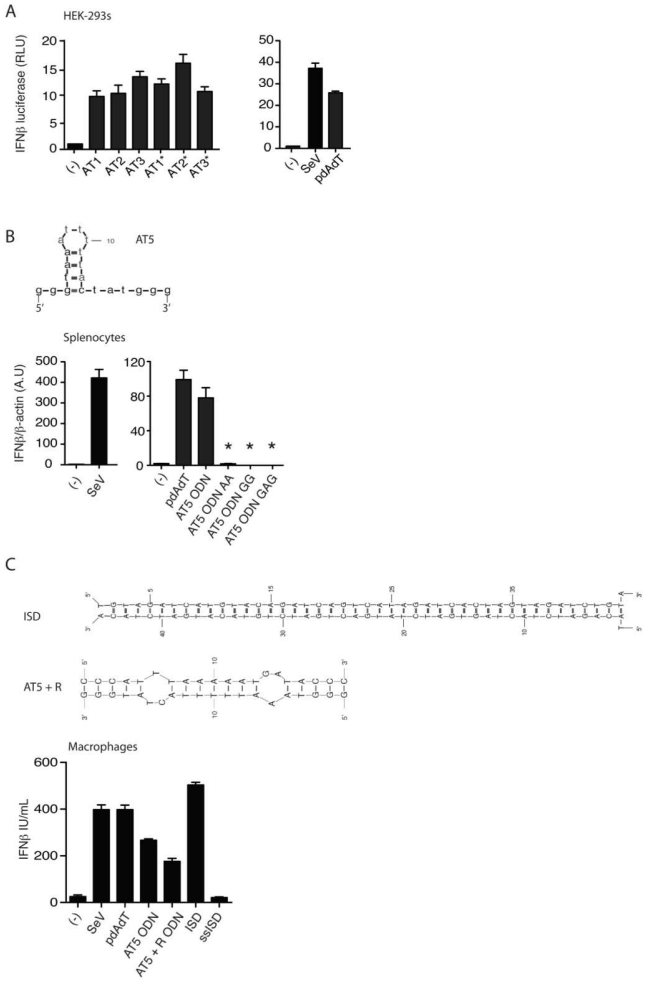

Figure 3. AT-rich motifs induce IFNβ production in a sequence and secondary structure-dependent manner

A. HEK293s transfected with the IFNβ reporter plasmid were stimulated with SeV, poly(dA-dT) and AT-rich ODN that were modified (*) as in Sup Fig. 2a and luciferase activity was read an additional 24h later. **B.** Putative secondary structure of AT-rich ODN AT5, with AT-motif and likely chief base-base interactions highlighted. Key base-base interaction and secondary structure was abolished by base-directed substitution of the original sequences as shown in Sup Fig. 2b. Splenocytes from C57BL/6 mice were stimulated with the parent AT5 (3μM, PD) and denoted base substituted oligonucleotides and IFNβ mRNA induction measured by qPCR. **C.** Predicted secondary structure of annealed AT-5 and reverse strand and ISD (3μM each, PD). BMDMs from C57BL/6 mice were stimulated with the ssAT5, AT5 annealed to its reverse strand (AT5 + R), annealed ISD and ssISD (forward strand only) for 18h and IFNβ secretion was measured by ELISA.

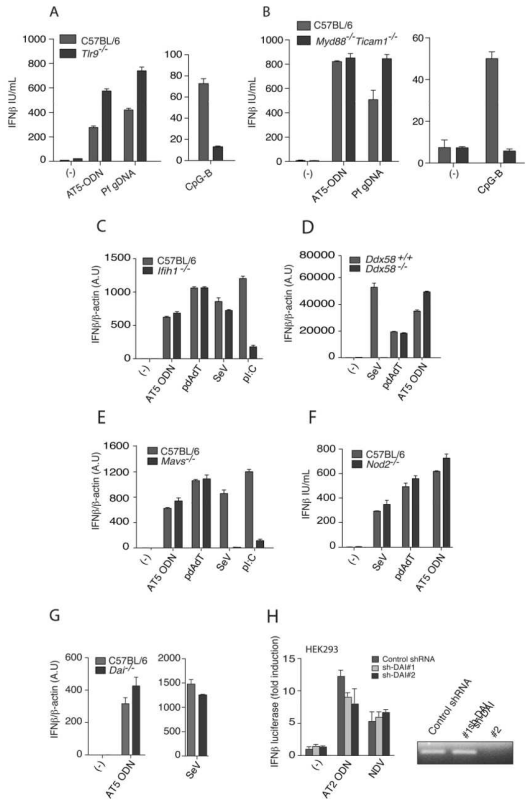

Figure 4. AT-rich DNA mediated IFNβ induction does not require TLRs, cytosolic sensors or the adaptor protein MAVS

A–B. Splenocytes from the indicated strains were stimulated with CpG-B 1826 (5μM), AT5 (3μM, PD) or with *Pf* 3D7 genomic DNA (100ng/ml) complexed with lipofectamine 2000 for 6h and IFNβ measured by qPCR and/or ELISA **C–G.** BMDMs from the indicated strains were stimulated with lipofectamine complexed AT5 (3μM, PD), poly (dA-dT) (5μg/ml), poly (I:C) (100ng/ml) or infected with SeV (200HAU/ml) and IFNβ mRNA measured by qPCR or ELISA. **H.** HEK293 cells were transduced with 2 lentiviruses encoding shRNA for DAI and IFNβ reporter gene activity measured measured from cells stimulated with lipofectamine complexed-AT2 (3μM, PS) or infected with NDV (80HAU/ml) for 24h. The efficiency of DAI silencing was examined by RT-PCR.

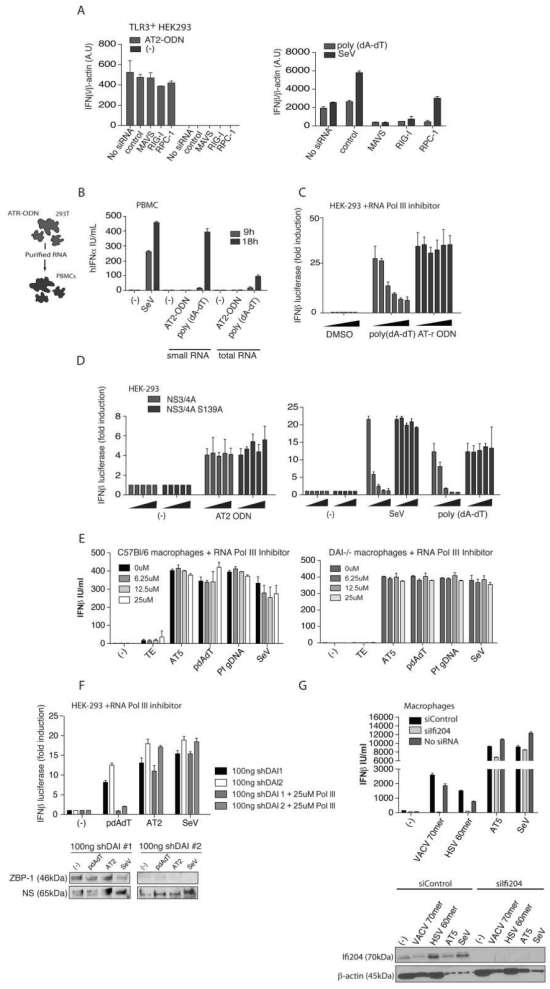

Figure 5. ***P. falciparum*** **AT-rich motifs do not signal via RNA-polymerase III/RIG-I**

A. RIG-I, MAVS and RNA polymerase III component 1 (RPC1) were silenced by RNAi. 48h later, cells were stimulated with AT2 (PS; left side of graphic), poly (dA-dT) and SeV (right side of graphic). IFNβ gene induction was assessed 24h later with qPCR **B.** HEK293 cells were transfected with either poly (dA-dT) or AT2 and RNA from the transfected cells was harvested 16 hr later. Harvested RNA was fractionated and purified as indicated and transfected back into PBMCs and IFNα production assessed 9 or 18h later. **C.** HEK293 cells were pre-treated with 0, 2.5, 5, 10, 20 or 30ng of the RNA polymerase III inhibitor, ML-60218 or vehicle alone (DMSO) for 2h and IFNβ reporter activity measured after AT2 (PS) or poly (dA-dT) treatment. **D.** 0, 20, 40, 60 and 80ng of plasmids encoding the Hepatitis C Virus (HCV) protease NS3/4A and the inactive mutant NS3/4A S139A were transfected into HEK293 cells along with the IFNβ reporter. 24h later the cells were stimulated with AT2 (PS), poly (dA-dT) and SeV. Luciferase activity was assessed a further 24 h later. **E.** C57Bl6 or DAI$^{-/-}$ macrophages were pretreated with ML-60218 for 2h and then stimulated as indicated and IFNβ levels measured by ELISA. **F.** DAI was silenced by RNAi and cells pretreated with the ML60218 inhibitor. IFNβ reporter gene activity measured after cells were stimulated with AT2, poly(dA-dT) and Sendai virus (SEV). shRNA mediated knockdown of DAI (ZBP-1) was assessed using western blotting at 48hrs after transfection of shRNAs. **G.** Mouse macrophages were electroporated with siRNA to Ifi204 or scrambled siRNA control for 48hrs and then stimulated with indicated ligands for a

further 24hrs. Supernatants were assessed for levels of IFNβ (top) by ELISA, while lysates of cells were assessed for levels of Ifi204 remaining (bottom) by western blotting.

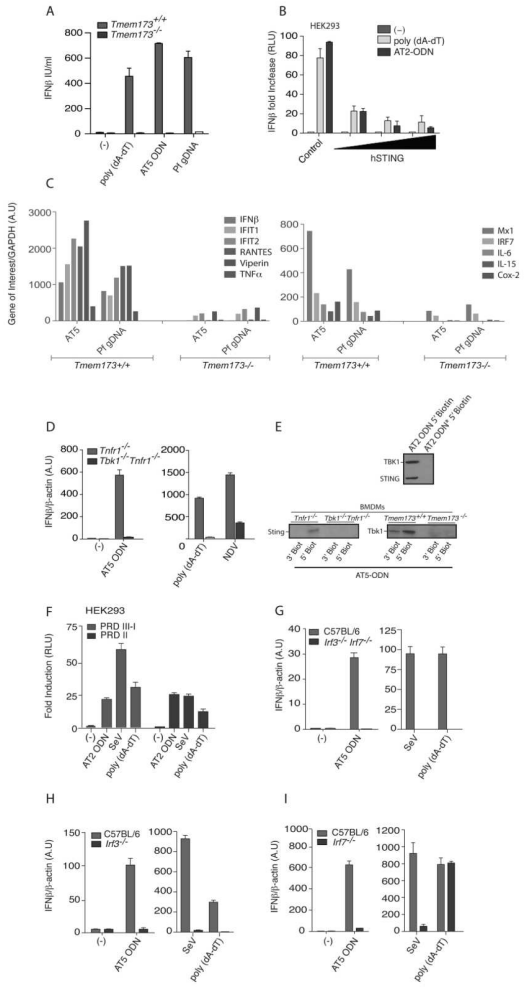

Figure 6. AT-rich DNA mediated IFNβ induction uses the adaptor STING, TBK1 and the interferon regulatory factors IRF3 and IRF7

A. BMDM from *Tmem173*$^{-/-}$ mice were transfected with lipofectamine complexed AT5 (3μM, PD), *Pf* 3D7 g DNA (*Pf* gDNA,100ng/ml), poly (dA-dT) (3.5μg/ml) or infected with SeV (200HAU/ml) and IFNβ gene induction measured 6h later by qPCR. **B.** STING was silenced by siRNA and IFNβ reporter gene activity measured after treatment with poly (dA-dT) and AT2. **C.** Bone marrow derived macrophages from *Tmem173*$^{+/+}$ and *Tmem173*$^{-/-}$ mice were stimulated as indicated for 6hrs and gene expression analyzed using Nano-string technology. **D.** *Tbk1*$^{-/-}$ *Tnfr1*$^{-/-}$ and *Tnfr1*$^{-/-}$ BMDM were treated as indicated and IFNβ mRNA levels measured by qPCR. **E.** HEK293 cells (upper panels) or BMDMs from *Tnfr1*$^{-/-}$, *Tbk1*$^{-/-}$ *Tnfr1*$^{-/-}$, *Tmem173*$^{+/+}$ and *Tmem173*$^{-/-}$ mice were transfected as indicated with biotinylated ODNs. Cell lysates were subjected to pull-down analysis and immunoblots were probed for the presence of Sting and TBK1 by western blotting. **F.** HEK293 cells were transfected with multimerized PRDIII-I and PRDII reporter elements from the IFNβ promoter and stimulated as above. Luciferase reporter activity was measured. **G–H.** BMDMs from *Irf3*$^{-/-}$ *Irf7*$^{-/-}$, *Irf3*$^{-/-}$ and *Irf7*$^{-/-}$ mice were transfected as indicated and levels of IFNβ mRNA were quantified 6h later by qPCR.

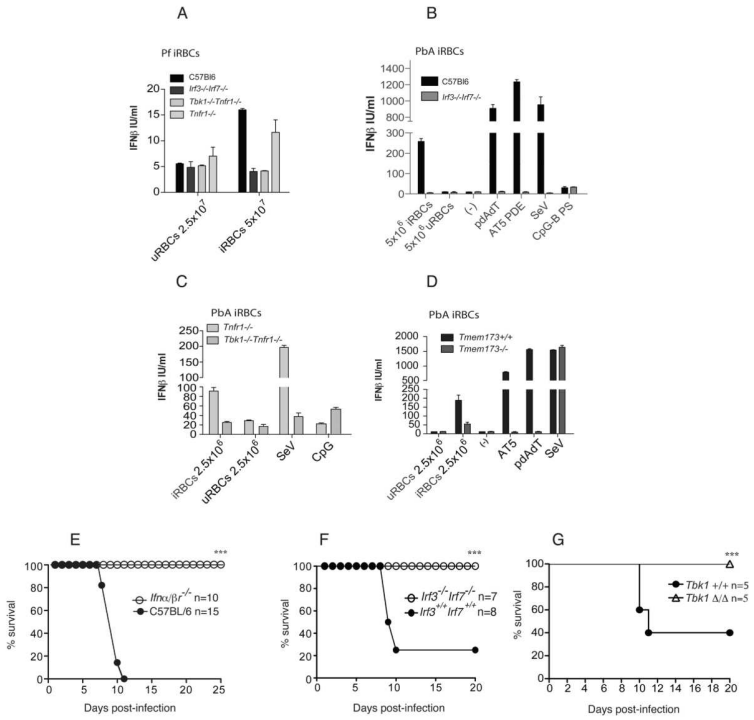

Figure 7. Role of STING, TBK1 and the transcription factors IRF3-IRF7 in Plasmodium induced IFN responses in vitro and in vivo

A. *Pf* infected RBCs (iRBCs) or uninfected RBCs (uRBCs) were incubated with C57Bl/6, *Irf3*$^{-/-}$*-Irf7*$^{-/-}$*, Tbk1*$^{-/-}$*-Tnfr1*$^{-/-}$ *and Tnfr1*$^{-/-}$ BMDMs as indicated **(B–D)**. *Plasmodium berghei* ANKA (PbA) iRBCs were incubated with BMDMs from Irf3$^{-/-}$-Irf7$^{-/-}$, Tbk1$^{-/-}$-Tnfr1$^{-/-}$, Tnfr1$^{-/-}$ and Tmem173$^{-/-}$ mice and IFNβ induction measured by ELISA. **(E–G)**. C57BL/6 (n=15), *Ifnar*$^{-/-}$ (n=10),, *Irf3*$^{-/-}$*/If7*$^{-/-}$ (n=7), *Irf3*$^{+/+}$*irf7*$^{+/+}$ (n=8), *Tbk1*$^{+/+}$ (n=5) and *Tbk1*Δ/Δ (n=5) mice were infected i.p. with 10^5 parasites of *P. berghei ANKA* strain and mice monitored daily for survival as shown. (*** $p \leq 0.0001$, student's t-test). A representative of three independent experiments is shown.